

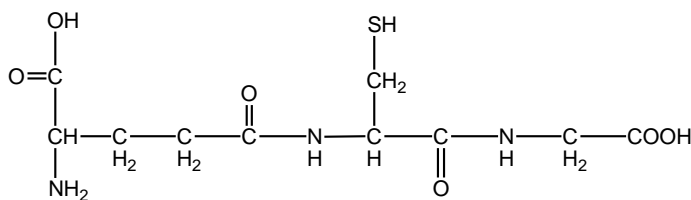
## Electronic Supplementary Information

### 1. Reagents

All the L-amino acids and L-glutathione (reduced form) were purchased from Sangon Biotch. Co. (Shanghai, China); Methyl orange, potassium tetrachloropalladate(II), 3-aminopropionic acid, tris(hydroxymethyl)aminomethane, 3,3'-dimethylglutaric acid, and the derivatives of anilines used, were purchased from Acros Organics Co., they were used without any further purification. All other reagents were of analytical grade or better and used without further purification.

MOP was prepared by a modified method of the literature<sup>[8]</sup>. In a typical preparation, methyl orange (0.2 mmol) and the stoichiometric amounts of potassium tetrachloropalladate(II) (0.4 mmol) were dissolved in a 30 mL dioxan/water (1:1) mixture and stirred at room temperature for a week. After the blue reaction mixture was concentrated to about 2 mL by rotary evaporation, the blue precipitate was collected and washed with ethanol and diethyl ether. The black solid was dried under vacuum to give 95 mg of MOP-2K (74% in yield).

L-glutathione was received as reduced form as illustrated below.



Structure of Glutathione

### 2. Characterization of MOP

#### (1) Mass spectrum (Figure 4) of MOP

The high-resolution mass spectrum of MOP (solvent: H<sub>2</sub>O) was measured on a Reflex III MALDI-TOF mass spectrometer (Bruker–Dalton Co., US; made in Germany). The main peak appearing at m/z 661 (1/2MOP+H<sub>2</sub>O) clearly confirmed the formation of MOP. MOP molecules were ruptured at the high-energy chloro-bridged Pd-Cl-Pd bonds during vaporization.

#### (2) FT-IR (Figure 5) of MOP

The  $\nu_{C-C}$  band of aromatic rings at  $1608\text{ cm}^{-1}$  of methyl orange was weakened and shifted to  $1595\text{ cm}^{-1}$  in the IR spectrum of MOP. Besides, the dense and strong absorbance usually appearing at  $1000\text{-}1200\text{ cm}^{-1}$ , which is characteristic of azo bond, was greatly weakened in the IR spectrum of MOP. Both confirmed the formation of cyclometalated metal-azo complex.

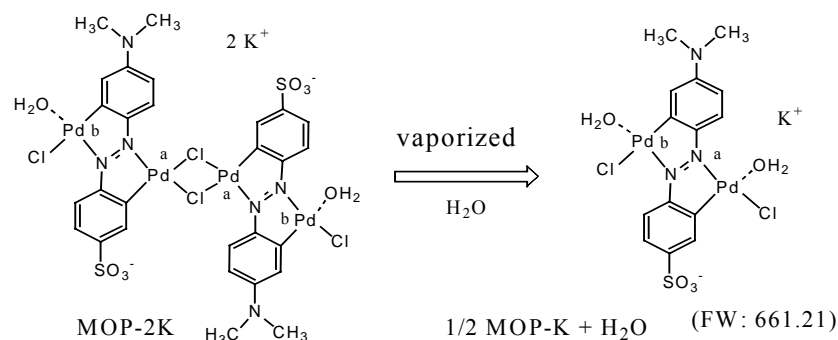
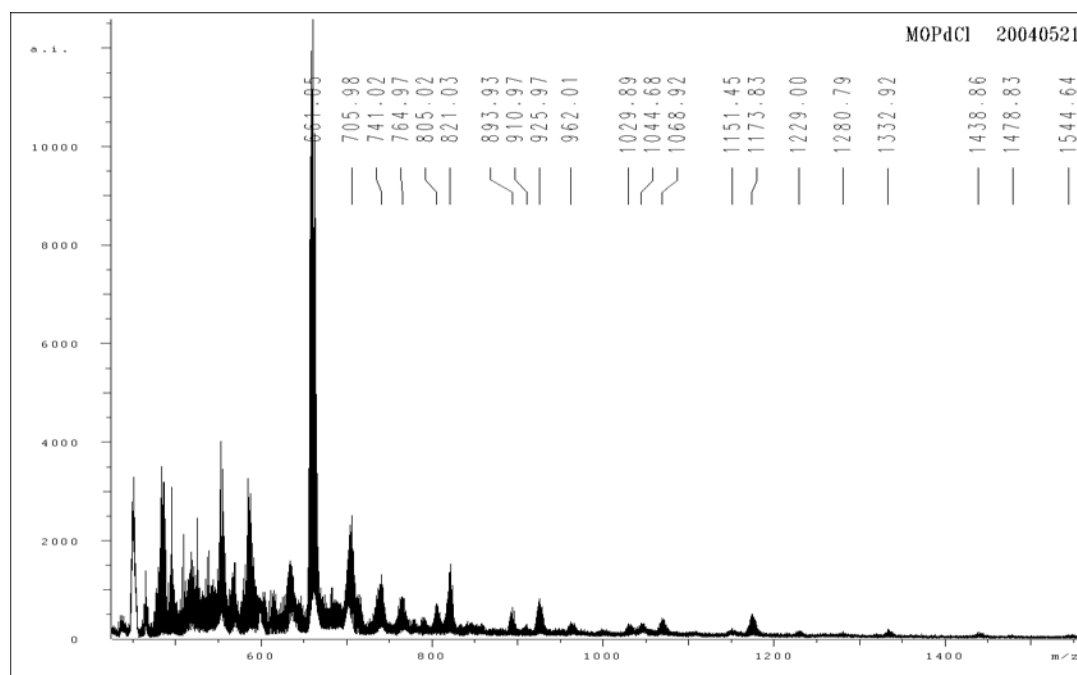


Figure 4. TOF-MS spectrum of MOP and its chemical illustration.

### (3) NMR spectra of MOP ( $^{13}\text{C}$ -NMR, Figure 6; $^1\text{H}$ -NMR, Figure 7)

The NMR spectra showed that the carbon and hydrogen atoms on the aromatic rings of methyl orange were placed in asymmetry after the palladium-azo cyclometallization. The  $^1\text{H}$ -NMR spectrum provided a more convicting proof for the formation of MOP-2K.  $^1\text{H}$ -NMR  $[(\text{D}_3\text{C})_2\text{SO}](500\text{ MHz})$ :  $\delta$  3.17 (s, 6H, N- $\text{CH}_3$ ); 6.62(d, 1H, Ph-H); 7.20 (s, 1H,

Ph-H); 7.29 (d, 1H, Ph-H); 7.91 (s, 1H, Ph-H); 8.20 (d, 1H, Ph-H); 8.50 (d, 1H, Ph-H); 2.5 (DMSO); 3.5 (H<sub>2</sub>O); 3.39 (s, 2H, Pd-OH<sub>2</sub>) .

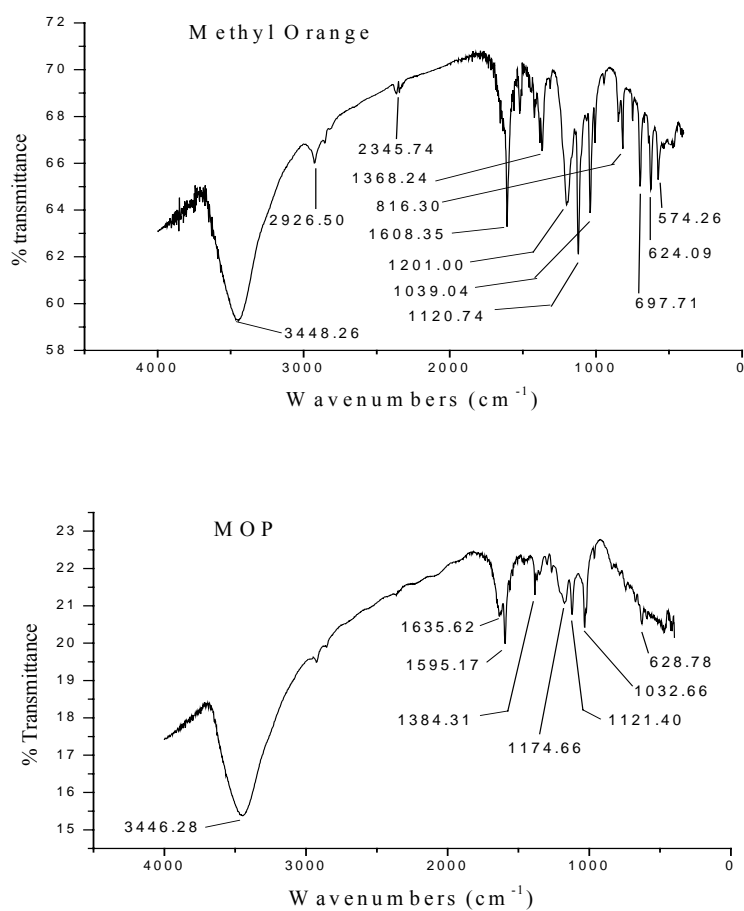


Figure 5. FT-IR spectra of methyl orange and MOP solids in KBr.

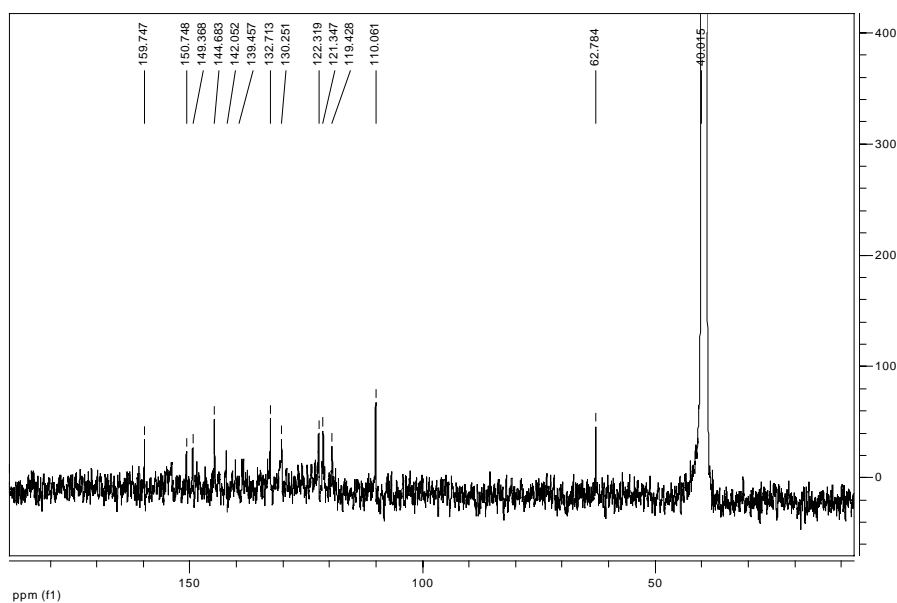


Figure 6.  $^{13}\text{C}$ -NMR spectrum of MOP.

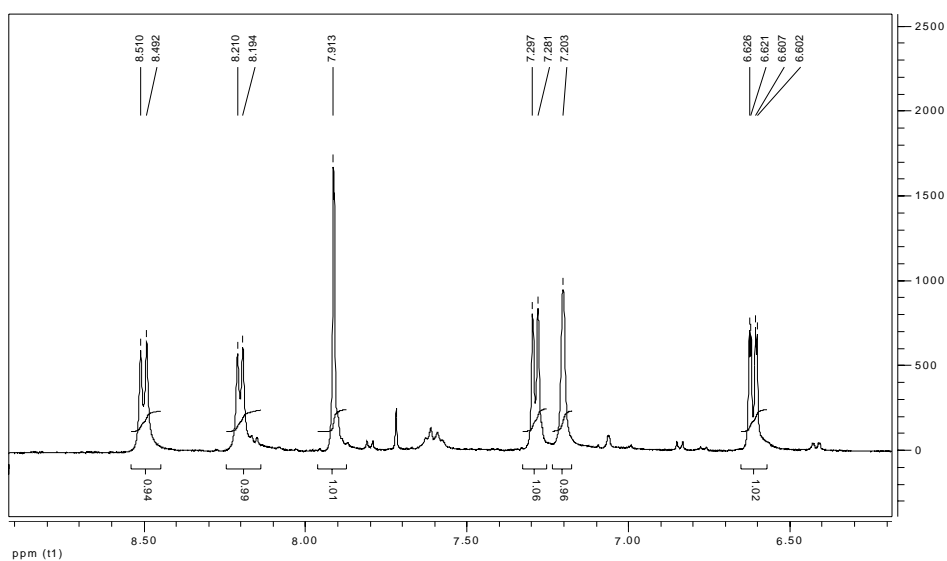
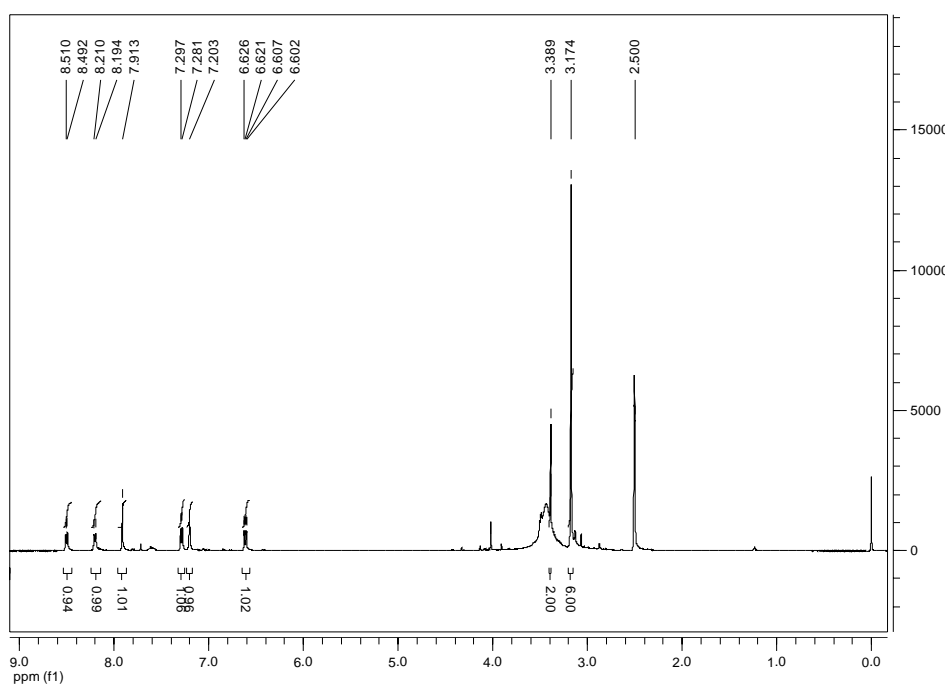


Figure 7.  $^1\text{H}$ -NMR spectrum of MOP.

(4) XPS spectra of MOP (Figure 8: a-total; b, Pd 3d ; c-Cl 2d)

The relative atom concentrations of C, N, O, S, Cl and Pd was calculated from the XPS spectra of MOP:  $n_{\text{C}} : n_{\text{N}} : n_{\text{O}} : n_{\text{S}} : n_{\text{Cl}} : n_{\text{Pd}} = 13:3:4:1:2:2$  (Figure 9a). Only Pd(II), no Pd(III)

or Pd(IV) was found in MOP (Figure 9b). The valence number of all the Cl atoms of MOP was  $-1$  as displayed by the XPS spectrum (Figure 9c).

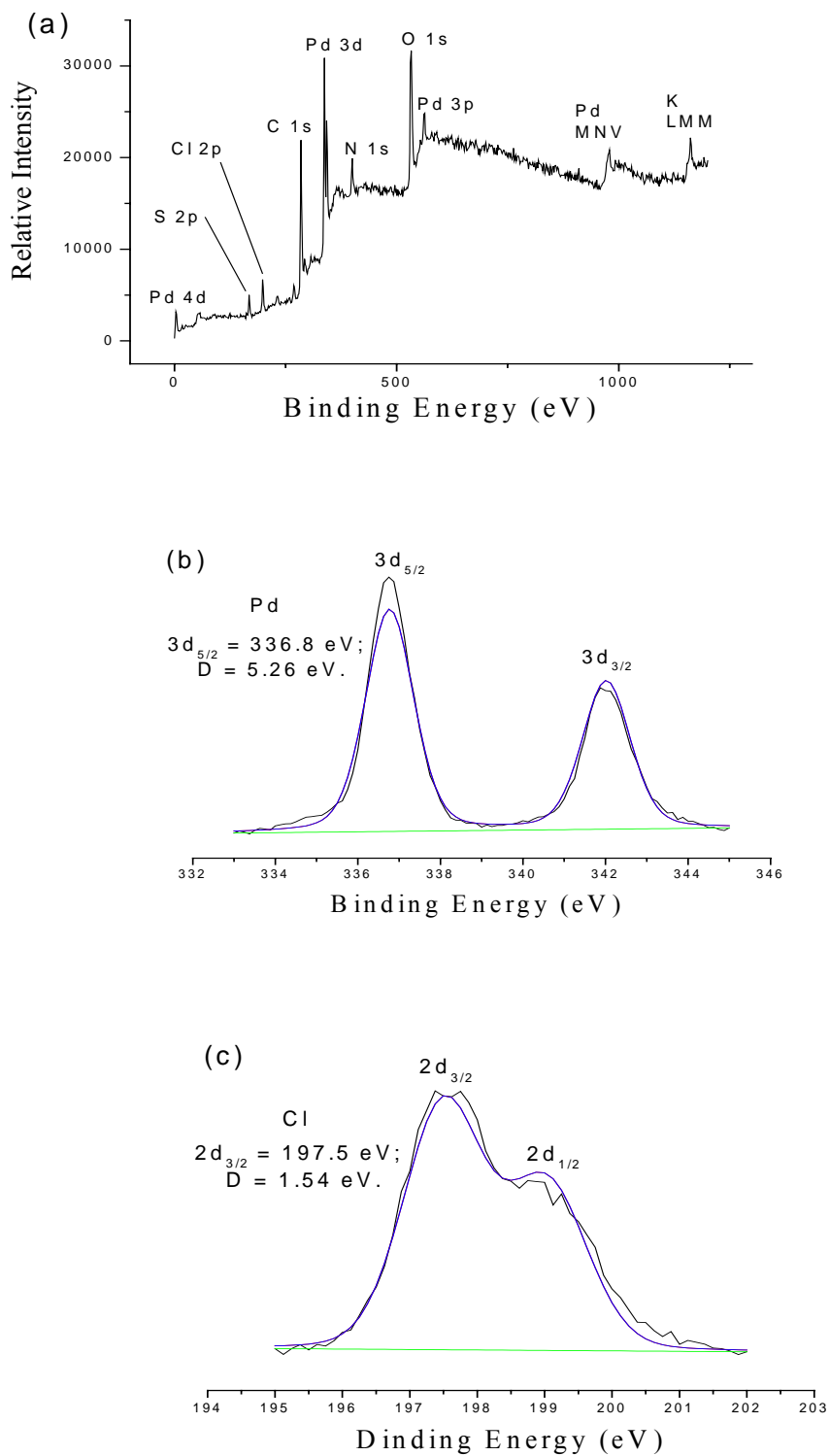


Figure 8. Total (a) and Pd 3d (b) and Cl 2d (c) XPS spectra of dried MOP solid.

### 3. Effect of pH on the sensing response (Figure 9)

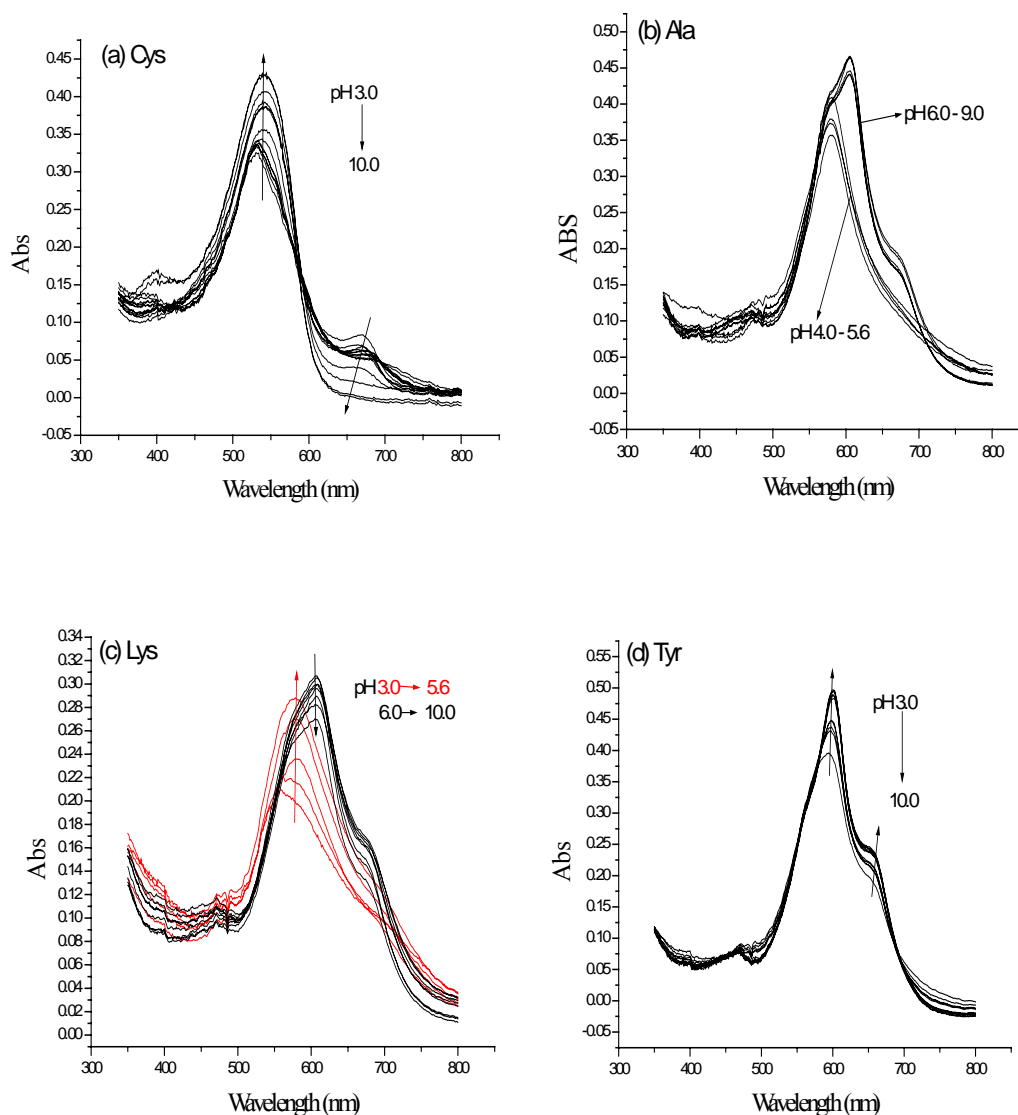


Figure 9. Effect of pH on the sensing responses of MOP ( $1.00 \times 10^{-5}$  M) towards different amino acids ( $2.00 \times 10^{-4}$  M). Buffer: pH 3.0-5.8, 0.02 M potassium biphthalates; pH 6.0-8.0, 0.02 M sodium phosphates; pH 9.2-10.0, 0.02 M sodium carbonates.

### 4. Differential UV-vis spectral responses of MOP to L- $\alpha$ -amino acids with different types of side chain groups in aqueous solution (Figure 10).

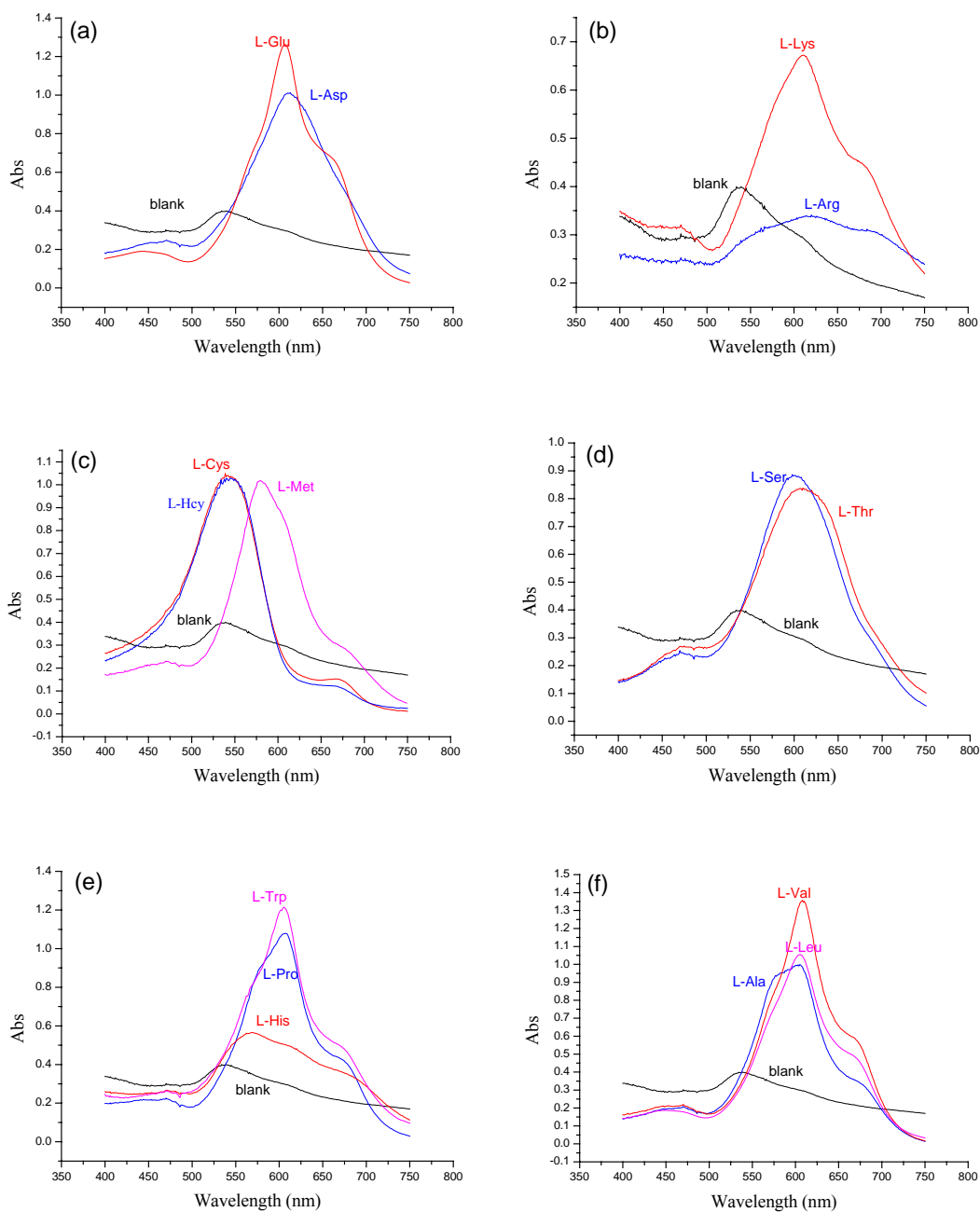


Figure 10. Absorption spectra of MOP sensing solutions ( $2.50 \times 10^{-5}$  M; buffered at pH 7.4 with 0.02 M phosphate buffer) in the presence of L-amino acids ( $4.00 \times 10^{-4}$  M) with different side chain groups: a) carboxyl-containing groups; b) basic groups; c) S-donor-containing groups; d) hydroxy-containing groups; e) heterocyclic rings; f) alkyl groups. Absorption spectra were recorded after 2-hour incubation in  $50^{\circ}\text{C}$  water bath.

##### 5. Effect of coexisting ions on the speed of sensing reactions (Figure 11)

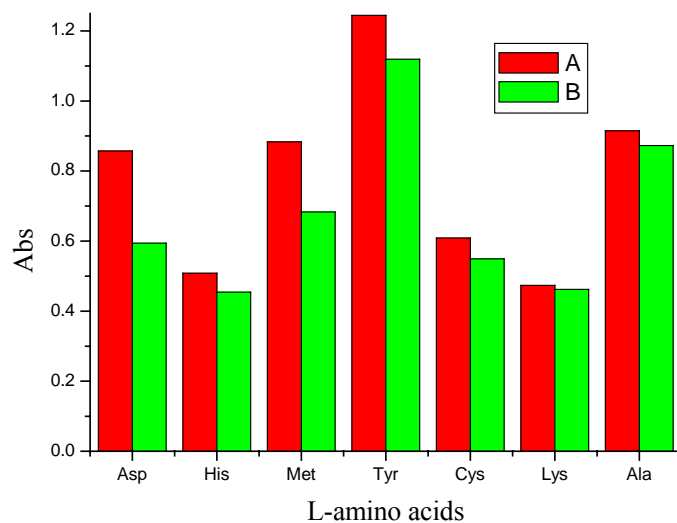


Figure 11. Absorbance values of MOP sensing solutions ( $2.00 \times 10^{-5}$  M, buffered at pH 7.4 with 0.02 M phosphate) reacted with different amino acids ( $8.00 \times 10^{-5}$  M) in the absence (A) and presence (B) of the mixed coexisting anions (0.10 M NaCl, 0.020 M  $\text{Na}_2\text{SO}_4$ , 0.030 M  $\text{NaHCO}_3$  and  $2.0 \times 10^{-3}$  M  $\text{NaNO}_3$ ) after 1-hour incubation in a  $50^\circ\text{C}$  water. Wavelengths at which absorbance were measured: Asp, 607nm; His, 559nm, Met, 577nm; tyr, 600nm; Cys, 550nm; Lys, 585nm; Ala, 603nm.